IEEE Access
Multidisciplinary | Rapid Review | Open Access Journal

Received August 25, 2018, accepted September 19, 2018, date of publication October 1, 2018, date of current version October 29, 2018.

Digital Object Identifier 10.1109/ACCESS.2018.2872732

S-Parameter Model of Three Parallel Interconnect Lines Generating Negative Group-Delay Effect

FAYU WAN[1], (Member, IEEE), NINGDONG LI[1], BLAISE RAVELO[2], (Member, IEEE), QIZHENG JI[3], AND JUNXIANG GE[1]

[1]Nanjing University of Information Science and Technology, Nanjing 210044, China
[2]Normandy University, UNIROUEN, ESIGELEC, IRSEEM EA 4353, Technopole du Madrillet, 76801 Saint Etienne du Rouvray, France
[3]Beijing Orient Institute of Measurement and Test, Beijing 100094, China

Corresponding author: Qizheng Ji (jiqizheng790308@sina.com)

This work was supported in part by NSFC under Grant 61601233 and Grant 61750110535, in part by the Electrostatic Research Foundation of Liu Shanghe Academicians and Experts Workstation, Beijing Orient Institute of Measurement and Test under Grant BOIMTLSHJD20181003, in part by the NSF of Jiangsu under Grant BK20150918, in part by the Jiangsu Innovation and Enterprise Group Talents Plan 2015 under Grant SRCB201526, and in part by PAPD.

ABSTRACT This paper develops a negative group-delay (NGD) microwave circuit theory regarding topology consists of three parallel interconnect lines (3-PILs). The NGD topology under study is built using completely distributed microstrip lines. The 3-PIL NGD theory is established from the S-parameters which are determined from the general admittance matrix of the 3-PILs. The analytical expressions of reflection coefficient (S_{11}), transmission coefficient (S_{21}) and group-delay (τ) which behave as periodical functions are presented. The frequency period proper to the 3-PIL topology is established. Then, S_{11}, S_{21} and τ illustrating the possibility to generate bandpass NGD function are formulated in function of the PIL parameter physical lengths and attenuation loss. Then, the NGD characterization of the 3-PIL topology is presented. The relevance of the NGD theory is verified with simulations and experimentations around the NGD center frequency of about 2.3 GHz. To do this, a 3-PIL microstrip circuit is designed and fabricated as proof-of-concept. It is shown that the simulated and measured group-delays are well-correlated. As expected theoretically, the demonstrator with identical characteristic impedance enables to generate an NGD level of approximately -2 ns at 2.3 GHz. In the future, the NGD function can be potentially used for the microwave signal integrity improvement.

INDEX TERMS Microwave circuit theory, distributed cell, negative group-delay (NGD), parallel interconnect line (PIL), S-parameter model.

I. INTRODUCTION

The functioning performance of all communication systems in different areas as in electronic, optical and electronic engineering depend implicitly on the signal delays [1]–[5]. Despite the communication system technological progress in term of operation speed and miniaturization, the undesirable influence of the signal delay remains an open issue for the design and fabrication engineers. Behind the design complexity, the signal delays remain one of the most significant problem of modern communication system [6].

A. DELAY EFFECT BIBLIOGRAPHIC ANALYSIS

In the area of RF and microwave engineering, the signal delays are mostly formulated by the group-delay which is analytically derived from the transmission phase $\phi(\omega)$ by the expression:

$$\tau(\omega) = -\frac{\partial\phi(\omega)}{\partial\omega}. \tag{1}$$

In addition to the noise effects, the group-delay limits considerably the performance of microwave devices [5], [7]. More generally, the time delay represents a main key parameter of signal integrity (SI) for different electronic system as the fanout of MOS integrated circuit (IC) [8], [9]. For several cases of implementation technology, the interconnect delay of CMOS circuit induces undesirable desynchronization problem [10], [11]. Because of desynchronizations, serial links may generate unintentionally information falsifications of digital and mixed data communication [12], [13]. To overcome this technical issue, different optimization techniques to reduce the interconnect delay were proposed. Most of the

digital circuit interconnects effect reduction techniques are based on the compensation techniques based on the use of repeaters [14], [15].

In RF and microwave engineering, the delay lines are regularly used to design different transceiver functions as phase shifters, filters and amplifiers [16]–[20]. Synthesis methods were developed in order to optimize the time-sharing between the different stages of the system [18]. The delay lines were exploited to implement a beam forming fan filters [19], frequency translator [20], channel blind identification [21], consensus of second order agents [22] and frequency doublers [23]. Nevertheless, so far, the RF and microwave design engineers are constantly looking for relevant techniques to reduce signal delay. One of the proposed and suitable solutions is the implementation of negative group-delay (NGD) function. In [24]–[26], the NGD circuit was inspired from negative refractive index metamaterials [24]–[26]. However, the NGD function remains so far, one of unfamiliar electronic functions. For the further understanding about this unfamiliar NGD function, a state of the art is presented in the next paragraph.

B. STATE OF THE ART ON THE NGD PHENOMENON

In the 1960s, the NGD phenomenon was initially found by Brillouin using dispersive and absorptive optical media [27]. It was demonstrated that the NGD phenomenon was observed around the resonance frequency of particular media. The observation can be understood with the absorptive media presenting refractive index $n(\omega)$ as a function of the angular frequency ω. In this situation, by denoting c the light speed in the vacuum, the group velocity of the media is given by:

$$v_g(\omega) = \frac{c}{\Re e\left[n(\omega) + \omega \cdot \frac{\partial n(\omega)}{\partial \omega}\right]}, \tag{2}$$

It is clear that the quantity v_g can be negative under the analytical condition:

$$\frac{\partial n(\omega)}{\partial \omega} < 0. \tag{3}$$

It means that the waves propagating through the structure having physical length d, which presents a group-delay equal to:

$$\tau = \frac{d}{v_g}, \tag{4}$$

becomes negative if $v_g < 0$. In 1970s, the NGD phenomenon was theoretically explained by Garret and McCamber with the pulse wave propagation through the media presenting group velocity expressed in (1) [28]. In 1980s, the NGD effect first experimentation was approved by Chu and Wong [29] and observed by Ségard and Macke [30] in optical wavelengths. More recently, the NGD phenomenon was experimented with electronic circuits [24]–[46]. At the beginning, the NGD electronic circuit was experimented with resonant lossy and low-frequency operational amplifier based active circuits. It was reported that the NGD behaviors of linear circuit are similar to the gain of liner filters [37]. Therefore, different categories of NGD function as low-pass, high-pass and bandpass circuits are identified. The bandpass NGD lumped circuits operate usually with resonator networks. It is noteworthy that the bandpass NGD circuits present asymptotic limits in function of the resonator parameters [38].

Nonetheless, by using electronic passive structures [24], [26] with the group-delay defined in (1). However, the generated NGD effect with passive circuit appears systematically with huge attenuation which can be more than 20 dB. By using lossy passive circuits, the NGD function was attempted to be used to design synthesizer and adjuster but the performances remain critical [32]–[34]. By using active topologies based on low frequency operational amplifiers, the circuits are limited by the NGD bandwidth, integration and power consumption. More recently, NGD topology of active circuit which uses RF transistor was developed [31]. As a result, to compensate the NGD circuit losses, the implementation with active circuits can be solutions [35], [36]. Some applications of NGD function were developed to design high performance phase shifters [39], [40], feedforward amplifiers [41], antennas [42] and a tentative study for the elimination of beam squint in serially fed antenna arrays [43].

Despite this trend of the interest, most of NGD active topologies are complex to design. Moreover, because of the use of lossy lumped inductor, the NGD active topologies cannot be integrated in high speed systems. As a result, simpler and low-loss passive topologies built with distributed transmission lines (TLs) were proposed [44]–[46]. These NGD distributed topologies are potentially integrable in high speed systems. However, the NGD distributed circuits require further research work because of the analytical theory complexity. For this reason, the present research work is focused on the NGD theory of distributed passive topology constituted by three parallel interconnect lines (3-PILs).

C. DESCRIPTION OF NOVELTY AND OUTLINE OF THE PAPER

In difference to research work proposed in [45], the proposed NGD topology consists of 3-PILs and the circuit theory is built with S-matrix modelling. The NGD analysis is performed in function of the electrical lengths and attenuation loss of constituting transmission lines (TLs).

For the better understanding, the paper is organized in three main sections. In Section II, the theoretical investigation is established. Based on the S-matrix analysis, the analytical characteristics of the PIL structure will be established from the transmission and reflection coefficients. It will be demonstrated that this fully distributed simple passive cell is capable to exhibit NGD phenomenon. To validate the bandpass NGD function, the design of validation prototypes will be described in Section III. Afterwards, the experimental test results compared with the theoretical calculations will be discussed. In Section IV, the paper will be ended by conclusion.

II. THEORETICAL INVESTIGATION

The present section describes the theoretical investigation of the proposed NGD PIL topology. The passive topology of PIL cell is described. The S-parameter modelling is developed from the PIL cell Y-matrix. Then, the NGD analysis is established.

A. TOPOLOGICAL DESCRIPTION

Fig. 1 introduces the topology of the PIL circuit. It acts as a two-port circuit. The analytical investigation of this topology institutes the key point of the present paper. The PIL topology consists of three lossy interconnect lines (ILs) $IL_k k = \{1, 2, 3\}$. The IL extremities are connected at the resistive sources V_1 and V_2. By denoting $j = \sqrt{-1}$ the complex number and ω is the angular frequency variable, the PIL S-parameter is modeled as:

$$[S_{PIL}(j\omega)] = \begin{bmatrix} S_{11}(j\omega) & S_{12}(j\omega) \\ S_{21}(j\omega) & S_{22}(j\omega) \end{bmatrix}. \quad (5)$$

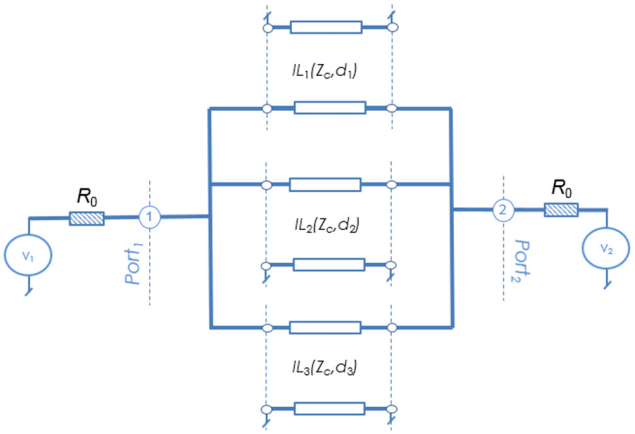

FIGURE 1. Topology of the three-IL based PIL structure.

Because of the PIL passive structure symmetry, we have the equality of reflection and transmission coefficients:

$$\begin{cases} S_{11}(j\omega) = S_{22}(j\omega) \\ S_{12}(j\omega) = S_{21}(j\omega). \end{cases} \quad (6)$$

To calculate this S-parameter model, the reference impedance Z_c is assimilated equal to $R_0 = 50\ \Omega$. The TL_k is defined by its characteristic impedance Z_k, attenuation a_k and physical length d_k. This former one is linked to the time delay by the relation:

$$\tau_k = \frac{d_k}{v}, \quad (7)$$

with v is the wave speed through the TL. The following analytical study is be realized by assuming that the ILs by their impedance matrices. The present study is focused on the case of PILs composed of only elementary three-ILs. It is noteworthy that the coupling effect between IL_k is out of the scope of the present study. The analytical model of the PIL topology will be explored in the next paragraph.

B. S-PARAMETER MODELLING OF THE PROPOSED PIL TOPOLOGY

Acting as a parallel type circuit topology, the modelling method of the 3-PIL structure should be intuitively realized with admittance or Y-matrix operation. Meanwhile, it is keen to restitute the ILs by their equivalent Y-matrices as depicted in Fig. 2(a). According to the TL theory, the Y-matrices of the ILs can be expressed as:

$$[Y_k(j\omega)] = \frac{1}{Z_k} \begin{bmatrix} \dfrac{a_k^2 + e^{-2j\omega\tau_k}}{a_k^2 - e^{-2j\omega\tau_k}} & \dfrac{-2a_k^2 e^{-2j\omega\tau_k}}{a_k^2 - e^{-2j\omega\tau_k}} \\ \dfrac{-2a_k^2 e^{-2j\omega\tau_k}}{a_k^2 - e^{-2j\omega\tau_k}} & \dfrac{a_k^2 + e^{-2j\omega\tau_k}}{a_k^2 - e^{-2j\omega\tau_k}} \end{bmatrix}, \quad (8)$$

with the subscript $k = \{1, 2, 3\}$.

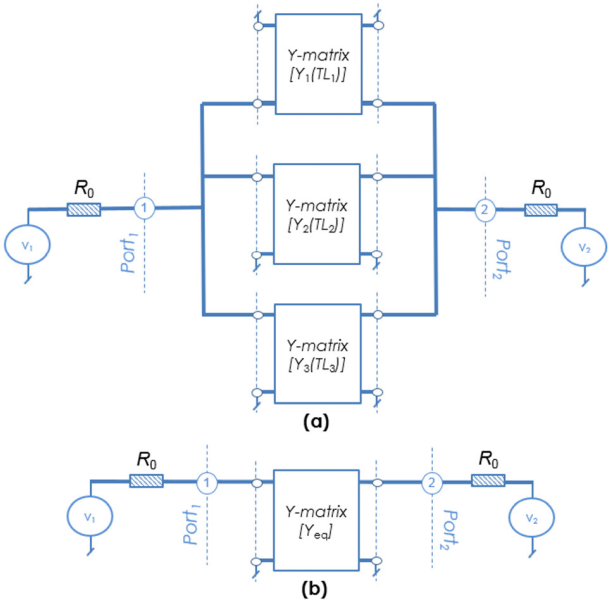

FIGURE 2. Equivalent topology of the PIL structure.

Therefore, the global circuit can be represented by the total admittance matrix as configured in Fig. 2(b). Based on the linear circuit and system theory, the equivalent PIL topology total Y-matrix is given by:

$$[Y_{PIL}(j\omega)] = [Y_1(j\omega)] + [Y_2(j\omega)] + [Y_3(j\omega)]. \quad (9)$$

The PIL S-matrix indicated in (5) is extracted from this global Y-matrix via the Y-to-S-matrix transform:

$$[S_{PIL}(j\omega)] = \begin{matrix} \{[Y_{PIL}(j\omega)]^{-1} - [Z]\} \times \\ \{[Y_{PIL}(j\omega)]^{-1} + [Z]\}^{-1}, \end{matrix} \quad (10)$$

with the reference impedance matrix:

$$[Z] = \begin{bmatrix} R_0 & 0 \\ 0 & R_0 \end{bmatrix}. \quad (11)$$

It is noteworthy that the 3-PIL S-parameter model developed in this paper is performed under the following hypotheses

related to the IL_k parameters:

$$\begin{cases} a_k = a, \\ Z_k = R_0 \\ \tau_2 = \tau_1, \\ \tau_0 = \tau_3 - \tau_1, \end{cases} \tag{12}$$

The frequency dependent reflection and transmission coefficients of the PIL are expressed as:

$$S_{11}(j\omega) = \frac{2\left[e^{j\omega(\tau_0+2\tau_1)} - a^2\right]^2}{\zeta(j\omega)}, \tag{13}$$

$$S_{21}(j\omega) = \frac{e^{j\omega\tau_1} a \begin{bmatrix} 2a^2(1+e^{j\omega\tau_0}) - e^{j\omega(\tau_0+2\tau_1)} \\ -2e^{2j\omega(\tau_0+\tau_1)} \end{bmatrix}}{\zeta(j\omega)}, \tag{14}$$

with:

$$\zeta(j\omega) = e^{2j\omega\tau_1}\left[a^2(4+e^{j\omega\tau_0}) - 4e^{2j\omega(\tau_0+\tau_1)}\right] - a^4. \tag{15}$$

Consequently, we get the S-parameter element magnitude and phase will be analytically examined in the frequency domain in the next paragraph.

C. FREQUENCY RESPONSES OF THE PIL TOPOLOGY

The frequency dependent magnitudes:

$$S_{11,12}(\omega) = \left|S_{11,12}(j\omega)\right|, \tag{16}$$

associated to the reflection and transmission coefficients described in (13) and (14) are respectively given by:

$$S_{11}(\omega) = \frac{2\left\{\begin{bmatrix}\cos[\omega(\tau_0+2\tau_1)] - a^2\end{bmatrix}^2 \\ +\sin^2[\omega(\tau_0+2\tau_1)]\right\}}{\zeta(\omega)}, \tag{17}$$

$$S_{21}(\omega) = \frac{\sqrt{\begin{Bmatrix} 2a^2(1+\cos(\omega\tau_0)) \\ -\cos[\omega(\tau_0+2\tau_1)] \\ -2\cos[2\omega(\tau_0+\tau_1)] \end{Bmatrix}^2 + \begin{Bmatrix} 2a^2\sin(\omega\tau_0) - \sin[\omega(\tau_0+2\tau_1)] \\ -2\sin[2\omega(\tau_0+\tau_1)] \end{Bmatrix}^2}}{\zeta(\omega)/a}, \tag{18}$$

with:

$$\zeta(\omega) = |\zeta(j\omega)| = \sqrt{\begin{Bmatrix} a^2\begin{bmatrix}4\cos(2\omega\tau_1) \\ +\cos[\omega(\tau_0+2\tau_1)]\end{bmatrix} \\ -4\cos[2\omega(\tau_0+2\tau_1)] - a^4 \end{Bmatrix}^2 + \begin{Bmatrix} a^2\begin{bmatrix}4\sin(2\omega\tau_1) \\ +\sin[\omega(\tau_0+2\tau_1)]\end{bmatrix} \\ -4\sin[2\omega(\tau_0+2\tau_1)] \end{Bmatrix}^2}. \tag{19}$$

The PIL reflection and transmission zeros are the roots of the following equation systems respectively:

$$\begin{cases} \cos[\omega(\tau_0+2\tau_1)] = a^2 \\ \sin[\omega(\tau_0+2\tau_1)] = 0, \end{cases} \tag{20}$$

$$\begin{cases} \begin{Bmatrix} 2a^2[1+\cos(\omega\tau_0)] \\ -\cos[\omega(\tau_0+2\tau_1)] \end{Bmatrix} = 2\cos[2\omega(\tau_0+\tau_1)] \\ 2a^2\sin(\omega\tau_0) - \sin[\omega(\tau_0+2\tau_1)] = 2\sin[2\omega(\tau_0+\tau_1)]. \end{cases} \tag{21}$$

The PIL transmission phase defined by:

$$\phi(\omega) = \arg[S_{21}(j\omega)], \tag{22}$$

can be written as:

$$\phi(\omega) = \phi_n(\omega) - \phi_d(\omega), \tag{23}$$

with:

$$\phi_n(\omega) = \arctan\left\{\frac{\begin{matrix}2a^2\sin(\omega\tau_0) - \sin[\omega(\tau_0+2\tau_1)] \\ -2\sin[2\omega(\tau_0+\tau_1)]\end{matrix}}{\begin{matrix}2a^2[1+\cos(\omega\tau_0)] \\ -\cos[\omega(\tau_0+2\tau_1)] \\ -2\cos[2\omega(\tau_0+\tau_1)]\end{matrix}}\right\}, \tag{24}$$

$$\phi_d(\omega) = \arctan\left\{\frac{\begin{matrix}a^2\begin{bmatrix}4\sin(2\omega\tau_1)+ \\ \sin[\omega(\tau_0+2\tau_1)]\end{bmatrix} \\ -4\sin[2\omega(\tau_0+2\tau_1)]\end{matrix}}{\begin{matrix}a^2\begin{bmatrix}4\cos(2\omega\tau_1)+ \\ \cos[\omega(\tau_0+2\tau_1)]\end{bmatrix} \\ -4\cos[2\omega(\tau_0+2\tau_1)] - a^4\end{matrix}}\right\}. \tag{25}$$

It yields the group-delay defined earlier in (4) can be formulated as:

$$\tau(\omega) = \tau_n(\omega) - \tau_d(\omega), \tag{26}$$

with:

$$\tau_n(\omega) = \frac{\begin{Bmatrix} 16a^2\begin{bmatrix}\cos[2\omega(\tau_0+\tau_1)]+ \\ \cos[\omega(\tau_0+2\tau_1)]\end{bmatrix} \\ +4a^2\cos(2\omega\tau_1) - 4(a^4+3)\cos(\omega\tau_0) \\ -5a^4 - 15 \end{Bmatrix}\tau_1 + \begin{Bmatrix} 8a^2\begin{bmatrix}\cos[2\omega(\tau_0+\tau_1)]+ \\ \cos[\omega(\tau_0+2\tau_1)]\end{bmatrix} \\ -9 - a^4 + 2(2a^4-3)\cos(\omega\tau_0) \end{Bmatrix}\tau_0}{\begin{matrix}5 + 4(a^4+1)\cos(\omega\tau_0) - 2a^2\cos(2\omega\tau_1) - 8a^2 \\ [\cos[2\omega(\tau_0+\tau_1)] + \cos[\omega(\tau_0+2\tau_1)]]\end{matrix}}, \tag{27}$$

and:

$$\tau_d(\omega) = \frac{\begin{matrix}4a^2(\tau_0+2\tau_1)\begin{Bmatrix}(a^4+12)\cos[\omega(\tau_0+2\tau_1)] \\ -2a^2\cos[2\omega(\tau_0+2\tau_1)]\end{Bmatrix} \\ +8a^2(\tau_0+\tau_1)\cos[2\omega(\tau_0+\tau_1)] \\ +2a^6\tau_1\cos(2\omega\tau_1) - 4a^4(\tau_0+4\tau_1)\cos(\omega\tau_0) \\ -2\left[8(a^4+2)\tau_0 + (17a^4+32)\tau_1\right]\end{matrix}}{\begin{matrix}8a^4\cos[2\omega(\tau_0+\tau_1)] - 2a^6\cos(2\omega\tau_1) \\ -8a^2\begin{Bmatrix}(a^4+4)\cos[\omega(\tau_0+2\tau_1)] \\ +a^2\cos[2\omega(\tau_0+\tau_1)]\end{Bmatrix} \\ +8a^4\cos(\omega\tau_0) + a^8 + 17a^4 + 16\end{matrix}}. \tag{28}$$

It can be noted out that because of the PIL distributed topology, the transmission coefficient magnitude and group-delay are periodical functions. The period must be associated to the term:

$$\tau_p = 3\tau_1 + 2\tau_0. \tag{29}$$

Let us analyze the behavior of these frequency responses at some particular frequencies in the paragraph.

D. NGD ANALYSIS

The NGD analysis consists in establishing the condition between the PIL parameters to get $\tau(\omega) < 0$.

Acting as a linear time-invariant system, there is a similarity between the behavior of the transmission coefficient magnitude expressed in (18) and the group-delay defined in (26). At very low frequency $\omega \approx 0$, it can be calculated that (17) and (18) become:

$$S_{11}(\omega \approx 0) = \frac{2(1-a^2)^2}{\left|a^4 - 5a^2 + 4\right|}, \tag{30}$$

$$S_{21}(\omega \approx 0) = \frac{3a(1-a^2)}{\left|a^4 - 5a^2 + 4\right|}. \tag{31}$$

Similarly, the analytical group-delay is written as:

$$\tau(\omega \approx 0) = \frac{(4+a^2)(3\tau_1 + \tau_0)}{3(4-a^2)}. \tag{32}$$

Being given that $a < 1$, this quantity is unconditionally positive. Therefore, the PIL topology should behave as a bandpass NGD function. For example, we can analyze the PIL responses at the angular frequency associated to the multiple of term:

$$\omega_p = \frac{3\pi}{3\tau_1 + 2\tau_0}. \tag{33}$$

The exact expressions of $S_{11}(\omega = \omega_p)$, $S_{21}(\omega = \omega_p)$ and $\tau(\omega = \omega_p)$ are analytically quite complicated. Let us denote:

$$x = \frac{\tau_0}{\tau_1}. \tag{34}$$

For the sake of mathematical simplification, we propose to proceed with the third order limited Maclaurin expansions of both numerator and denominator quantities with respect to the quantity x:

$$S_{11}(\omega_p, x) \approx \frac{N_{11}(\omega_p) + \dot{N}_{11}(\omega_p)x + \frac{\ddot{N}_{11}(\omega_p)}{2}x^2 + O(x^3)}{D_{11}(\omega_p) + \dot{D}_{11}(\omega_p)x + \frac{\ddot{D}_{11}(\omega_p)}{2}x^2 + O(x^3)}, \tag{35}$$

$$S_{21}(\omega_p, x) \approx \frac{N_{21}(\omega_p) + \dot{N}_{21}(\omega_p)x + \frac{\ddot{N}_{21}(\omega_p)}{2}x^2 + O(x^3)}{D_{21}(\omega_p) + \dot{D}_{21}(\omega_p)x + \frac{\ddot{D}_{21}(\omega_p)}{2}x^2 + O(x^3)}, \tag{36}$$

$$\tau(\omega_p, x) \approx \frac{N_\tau(\omega_p) + \dot{N}_\tau(\omega_p)x + \frac{\ddot{N}_\tau(\omega_p)}{2}x^2 + O(x^3)}{D_\tau(\omega_p) + \dot{D}_\tau(\omega_p)x + \frac{\ddot{D}_\tau(\omega_p)}{2}x^2 + O(x^3)}. \tag{37}$$

It yields the following expressions:

$$S_{11}(\omega_p, x) \approx \left| \frac{4(1-a^2)\left[a^2(\pi^2x^2 - 18) + 9(a^4+1)\right]}{\pi^2(105a^2 - 64 - 29a^4)x^2 + 144 - 216a^2 + 81a^4 - 9a^6} \right|, \tag{38}$$

$$S_{21}(\omega_p, x) \approx \left| \frac{a^2(1-a^2)(2\pi^2x^2 - 9)}{\pi^2(105a^2 - 64 - 29a^4)x^2 + 144 - 216a^2 + 81a^4 - 9a^6} \right|, \tag{39}$$

$$\tau(\omega_p, x) = \frac{81\tau_1 \left\{ \begin{matrix} \pi^2(16 - 32a^2 + 21a^4 + 2a^6 - a^8)x^2 \\ -9(1-a^2)^2(16 - a^4)(9 + 3x) \end{matrix} \right\}}{2\pi^2(144 - 504a^2 + 531a^4 - 180a^6 + 9a^8)x^2 - 1296 + 3240a^2 - 2673a^4 + 810a^6 - 81a^8}. \tag{40}$$

The NGD existence condition derived from the last equation is given by:

$$\begin{cases} x^2 \leq \dfrac{9(1-a^2)^2(16-a^4)(9+3x)}{\pi^2(16 - 32a^2 + 21a^4 + 2a^6 - a^8)} \\ x^2 > \dfrac{1296 - 3240a^2 + 2673a^4 - 810a^6 + 81a^8}{2\pi^2(144 - 504a^2 + 531a^4 - 180a^6 + 9a^8)}, \end{cases} \tag{41}$$

or:

$$\begin{cases} x^2 \geq \dfrac{9(1-a^2)^2(16-a^4)(9+3x)}{\pi^2(16 - 32a^2 + 21a^4 + 2a^6 - a^8)} \\ x^2 < \dfrac{1296 - 3240a^2 + 2673a^4 - 810a^6 + 81a^8}{2\pi^2(144 - 504a^2 + 531a^4 - 180a^6 + 9a^8)}. \end{cases} \tag{42}$$

To validate the established NGD theory, simulation and measurement results will be discussed in the next section.

III. SIMULATION AND EXPERIMENTAL VALIDATIONS WITH MICROSTRIP PILs

As application of the previous theory, a POC of PIL prototype design and fabrication is described in the next paragraph. Then, the theoretical, simulated and experimental S-parameters and group delays will be compared.

A. PIL POC DESCRIPTION

To validate experimentally the innovative NGD PIL topology, a microstrip circuit prototype is designed and fabricated. The circuit under test (CUT) prototype is displayed in Fig. 3. The 3D design presented in Fig. 3(a) was realized in the HFSS® environment. Fig. 3(b) depicts the photograph of the fabricated CUT. It presents the physical sizes 38 mm × 24 mm.

This NGD PIL demonstrator is implemented with passive circuits in fully distributed microstrip technology.

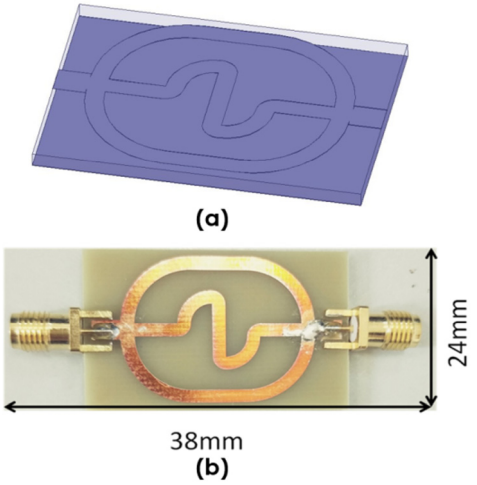

FIGURE 3. (a) HFSS 3D design and (b) photograph of the tested POC PIL prototype.

The CUT was implemented on FR4-epoxy substrate with relative permittivity $\varepsilon_r = 4.8$ and thickness $h = 1.6$ mm. The dielectric substrate was Cu-metallized with conductor thickness $t = 35$ μ m. The CUT is a transmission type PIL composed of microstrip ILs having width $w = 2.8$ mm and having different physical lengths $d_1 = d_2 = 30.7$ mm and $d_3 = 36$ mm. It corresponds to the time delays respectively of about $\tau_1 \approx 194$ ps and $\tau_2 \approx 228$ ps. The TLs characteristic impedances are equal to R_0.

B. VALIDATION MASURED RESULTS

The transmission and reflection coefficients and the group-delay measurements were carried out in order to confirm experimentally the NGD existence with the PIL structure. The experimental setup configuration with the CUT and the vector network analyzer (VNA) is shown in Fig. 4.

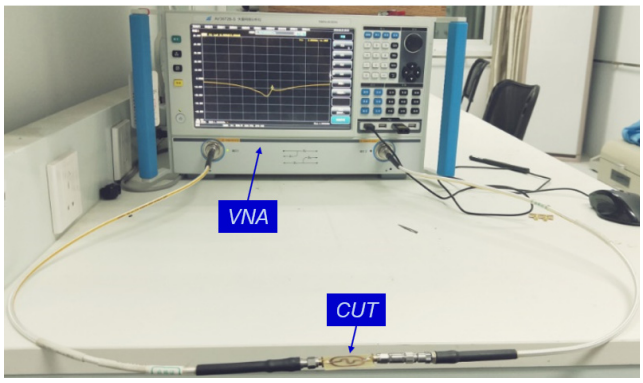

FIGURE 4. Configuration of the S-parameter measurement experimental setup.

The simulation and measurements are carried out from 2.2 GHz to 2.4 GHz. For the sake of brevity, only the narrow band aspect showing the circuit behavior in the NGD frequency band is analyzed in this paper. The comparison between the simulated (“simu.”), modelled and measured (“meas.”) group-delay responses from the CUT introduced in Fig. 3 is plotted in Fig. 5. As expected, the tested circuits confirm the possibility to exhibit the bandpass NGD function. At the center or optimal frequency of about $f_p \approx 2.3$ GHz from (29) in theory and 2.29 GHz in measurement, an NGD with optimal peak of about -2.26 ns in model, -1.8 ns in simulation and -2.59 ns in measurement was observed. Furthermore, the PIL CUT presents an NGD bandwidth of about 36 MHz.

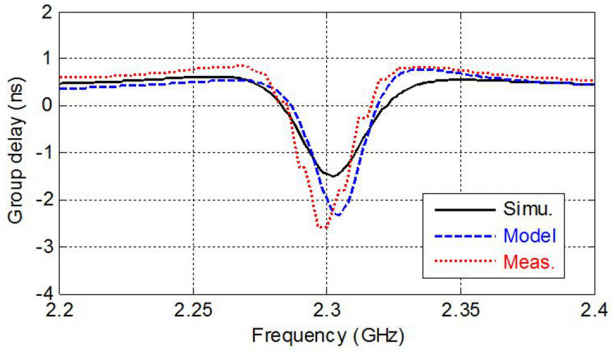

FIGURE 5. Group-delay responses of the PIL prototype shown in Fig. 3.

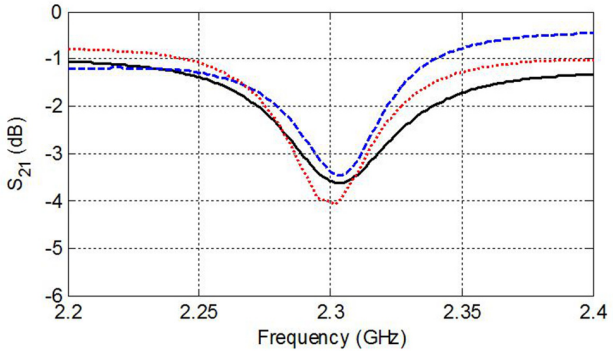

FIGURE 6. Transmission coefficient of the PIL prototype shown in Fig. 3.

Moreover, as can be seen in Fig. 6, the PIL presents maximal attenuation of only -3.4 dB in theory and -4.1 dB

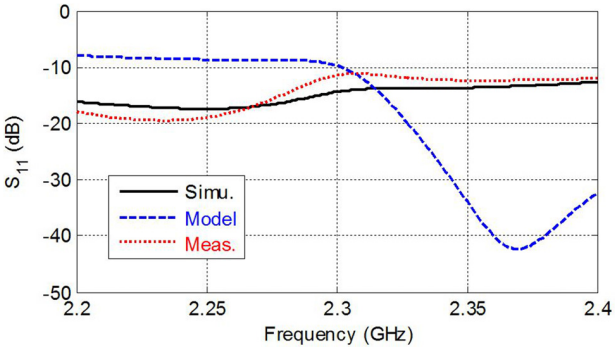

FIGURE 7. Reflection coefficient of the PIL prototype shown in Fig. 3.

in measurement around the center frequency. The obtained NGD levels and insertion losses which are better than −2 ns and −10dB are very interesting compared to the passive parts of the NGD circuits proposed in [24], [26], [42], and [44]. Furthermore, the measured reflection coefficient is plotted in Fig. 7. It can be observed once again that the tested circuit exhibits the return loss better than 12 dB. The slight NGD central frequency shift between the theoretical and measurement results is due to the inaccuracies of the considered dielectric substrate effective permittivity and losses compared to the simulated parameters.

IV. CONCLUSION

A microwave circuit theory of passive topology consisted of 3-PILs is developed.

The main parameters of the PIL structure are the TL attenuation loss and physical lengths. The equivalent Y-matrix of the PIL cell is established. The NGD analysis and characterization is elaborated from the S-parameter modelling. The analytical expressions of transmission and reflection coefficients and group-delay are expressed in function of the frequency. It was established that the 3-PIL topology present a particular frequency period in function of the physical lengths of TLs constituting the PIL. It was demonstrated that this simple distributed PIL is susceptible to generate NGD phenomenon.

The established theory of NGD PIL was validated by designing and fabricating a microstrip circuit prototype. The designed, simulated and tested PIL prototype is composed of three ILs having same impedance characteristic lines and having different physical lengths. As predicted in theory, group delay response presenting a bandpass NGD behavior is observed. It was shown that the calculated, simulated and measured S-parameters and group-delays are in very good agreement. An NGD of about −2.3 ns was observed at the frequency center 2.3 GHz with attenuation loss of about −3.5 dB. The PIL prototype operates with NGD bandwidth of about 36 MHz.

The NGD PIL topology presents a possibility to operate at higher frequencies size up to several ten GHz. Thanks to the design simplicity and its potential integration, the NGD PIL topology can be a good candidate for the reduction of signal delays in high speed digital and mixed electronic systems.

REFERENCES

[1] M. Rodriguez, R. Williams, and T. Carlow, "Signal delay and waveform estimation using unwrapped phase averaging," *IEEE Trans. Acoust., Speech, Signal Process.*, vol. ASSP-29, no. 3, pp. 508–513, Jun. 1981.

[2] M. S. Brandstein and H. F. Silverman, "A robust method for speech signal time-delay estimation in reverberant rooms," in *Proc. IEEE Int. Conf. Acoust., Speech, Signal Process. (ICASSP)*, Munich, Germany, vol. 1, Apr. 1997, pp. 375–378.

[3] M. Fukazawa and M. Nagata, "Measurements of digital signal delay variation due to dynamic power supply noise," in *Proc. IEEE Asian Solid-State Circuits Conf.*, Hsinchu, Taiwan, Nov. 2005, pp. 165–168.

[4] G. Lenz, B. J. Eggleton, C. K. Madsen, and R. E. Slusher, "Optical delay lines based on optical filters," *IEEE J. Quantum Electron.*, vol. 37, no. 4, pp. 525–532, Apr. 2001.

[5] E. Janssen *et al.*, "Fully balanced 60 GHz LNA with 37 % bandwidth, 3.8 dB NF, 10 dB gain and constant group delay over 6 GHz bandwidth," in *Proc. Top. Meeting Silicon Monolithic Integr. Circuits RF Syst. (SiRF)*, New Orleans, LA, USA, Jan. 2010, pp. 124–127.

[6] S.-S. Myoung, B.-S. Kwon, Y.-H. Kim, and J.-G. Yook, "Effect of group delay in RF BPF on impulse radio systems," *IEICE Trans. Commun.*, vol. E90-B, no. 12, pp. 3514–3522, 2007.

[7] G. Groenewold, "Noise and group delay in active filters," *IEEE Trans. Circuits Syst. I, Reg. Papers*, vol. 54, no. 7, pp. 1471–1480, Jul. 2007.

[8] J. Rubinstein, P. Penfield, and M. A. Horowitz, "Signal delay in RC tree networks," *IEEE Trans. Comput.-Aided Des. Integr. Circuits Syst.*, vol. CAD-2, no. 3, pp. 202–211, Jul. 1983.

[9] P. K. Chan and K. Karplus, "Computing signal delay in general RC networks by tree/link partitioning," in *Proc. 26th ACM/IEEE Conf. Design Autom.*, Las Vegas, NV, USA, Jun. 1989, pp. 485–490.

[10] M. E. Hwang, S. O. Jung, and K. Roy, "Slope interconnect effort: Gate-interconnect interdependent delay modeling for early CMOS circuit simulation," *IEEE Trans. Circuits Syst. I, Reg. Papers*, vol. 56, no. 7, pp. 1428–1441, Jul. 2009.

[11] T. J. Brazil, "Nonlinear, transient simulation of distributed RF circuits using discrete-time convolution," in *Proc. IEEE Int. Symp. Circuits Syst. (ISCAS)*, New Orleans, LA, USA, May 2007, pp. 505–508.

[12] M. Ghoneima, Y. Ismail, M. M. Khellah, J. Tschanz, and V. De, "Serial-link bus: A low-power on-chip bus architecture," *IEEE Trans. Circuits Syst. I, Reg. Papers*, vol. 56, no. 9, pp. 2020–2032, Sep. 2009.

[13] Y. Bai and S. S. Wong, "Optimization of driver preemphasis for on-chip interconnects," *IEEE Trans. Circuits Syst. I, Reg. Papers*, vol. 56, no. 9, pp. 2033–2041, Sep. 2009.

[14] M. Bartolini, P. Pulici, P. P. Stoppino, G. Campardo, and G. P. Vanalli, "A reduced output ringing CMOS buffer," *IEEE Trans. Circuits Syst., II, Exp. Briefs*, vol. 54, no. 2, pp. 102–106, Feb. 2007.

[15] F. R. Awwad, M. Nekili, V. Ramachandran, and M. Sawan, "On modeling of parallel repeater-insertion methodologies for SoC interconnects," *IEEE Trans. Circuits Syst. I, Reg. Papers*, vol. 55, no. 1, pp. 322–335, Feb. 2008.

[16] E. C. Heyde, "Theoretical methodology for describing active and passive recirculating delay line systems," *Electron. Lett.*, vol. 31, no. 23, pp. 2038–2039, Nov. 1995.

[17] I. M. Filanovsky, "One method of synthesis of time delay circuits," in *Proc. 42nd Midwest Symp. Circuits Syst.*, Las Cruces, NM, USA, vol. 2, Aug. 1999, pp. 1032–1035.

[18] H. F. Li, S. C. Leung, and P. N. Lam, "Optimised synthesis of delay-insensitive circuits using time-sharing," *IEE Proc.-Comput. Digit. Techn.*, vol. 141, no. 2, pp. 111–118, Mar. 1994.

[19] C. Wijenayake, Y. Xu, A. Madanayake, L. Belostotski, and L. T. Bruton, "RF analog beamforming fan filters using CMOS all-pass time delay approximations," *IEEE Trans. Circuits Syst. I, Reg. Papers*, vol. 59, no. 5, pp. 1061–1073, May 2012.

[20] G. Agrawal, S. Aniruddhan, and R. K. Ganti, "Multi-band RF time delay element based on frequency translation," in *Proc. IEEE Int. Symp. Circuits Syst. (ISCAS)*, Melbourne, VIC, Australia, Jun. 2014, pp. 1368–1371.

[21] S. V. Narasimhan, M. Hazarathaiah, and P. V. S. Giridhar, "Channel blind identification based on cyclostationarity and group delay," *Signal Process.*, vol. 85, no. 7, pp. 1275–1286, Jul. 2005.

[22] R. Cepeda-Gomez and N. Olgac, "Consensus of a group of second order agents with switching irregular communication topologies and time-delay," in *Proc. 49th IEEE Conf. Decis. Control (CDC)*, Atlanta, GA, USA, Dec. 2010, pp. 5474–5479.

[23] B. R. Jackson and C. E. Saavedra, "An L-band CMOS frequency doubler using a time-delay technique," in *Top. Meeting Silicon Monolithic Integr. Circuits RF Syst. Dig. Papers*, San Diego, CA, USA, Jan. 2006, p. 4.

[24] L. Markley and G. V. Eleftheriades, "Quad-band negative-refractive-index transmission-line unit cell with reduced group delay," *Electron. Lett.*, vol. 46, no. 17, pp. 1206–1208, Aug. 2010.

[25] S. J. Erickson, M. Khaja, and M. Mojahedi, "Time- and frequency-domain measurements for an active negative group delay circuit," in *Proc. IEEE Antennas Propag. Soc. Int. Symp.*, Washington, DC, USA, vol. 3A, Jul. 2005, pp. 790–793.

[26] J. N. Munday and W. M. Robertson, "Observation of negative group delays within a coaxial photonic crystal using an impulse response method," *Opt. Commun.*, vol. 273, no. 1, pp. 32–36, 2007.

[27] L. Brillouin, *Wave Propagation and Group Velocity*. New York, NY, USA: Academic, 1960.

[28] C. G. B. Garrett and D. E. McGumber, "Propagation of a Gaussian light pulse through an anomalous dispersion medium," *Phys. Rev. A, Gen. Phys.*, vol. 1, pp. 305–313, Feb. 1970.
[29] S. Chu and S. Wong, "Linear pulse propagation in an absorbing medium," *Phys. Rev. Lett.*, vol. 48, pp. 738–741, Mar. 1982.
[30] B. Segard and B. Macke, "Observation of negative velocity pulse propagation," *Phys. Lett. A*, vol. 109, pp. 213–216, May 1985.
[31] B. Ravelo, "Neutralization of LC- and RC-disturbances with left-handed and NGD effects," *Adv. Electromagn.*, vol. 2, no. 1, pp. 73–84, Oct. 2013.
[32] K.-P. Ahn, R. Ishikawa, A. Saitou, and K. Honjo, "Synthesis for negative group delay circuits using distributed and second-order RC circuit configurations," *IEICE Trans. Electron.*, vol. E92-C, no. 9, pp. 1176–1181, 2009.
[33] S. Park, H. Choi, and Y. Jeong, "Microwave group delay time adjuster using parallel resonator," *IEEE Microw. Wireless Compon. Lett.*, vol. 17, no. 2, pp. 109–111, Feb. 2007.
[34] K.-J. Song, S.-G. Kim, H.-J. Choi, and Y.-C. Jeong, "Group delay time matched CMOS microwave frequency doubler," *J. Korean Inst. Electromagn. Eng. Sci.*, vol. 19, no. 7, pp. 771–777, 2008.
[35] M. Kandic and G. E. Bridges, "Bilateral gain-compensated negative group delay circuit," *IEEE Microw. Wireless Compon. Lett.*, vol. 21, no. 6, pp. 308–310, Jun. 2011.
[36] F. Wan, N. Li, B. Ravelo, Q. Ji, B. Li, and J. Ge, "The design method of the active negative group delay circuits based on a microwave amplifier and an RL-series network," *IEEE Access*, vol. 6, pp. 33849–33858, Jun. 2018.
[37] B. Ravelo, "Similitude between the NGD function and filter gain behaviours," *Int. J. Circuit Theory Appl.*, vol. 42, no. 10, pp. 1016–1032, Oct. 2014.
[38] M. Kandic and G. E. Bridges, "Asymptotic limits of negative group delay in active resonator-based distributed circuits," *IEEE Trans. Circuits Syst. I, Reg. Papers*, vol. 58, no. 8, pp. 1727–1735, Aug. 2011.
[39] S. Keser and M. Mojahedi, "Broadband negative group delay microstrip phase shifter design," in *Proc. IEEE Antennas Propag. Soc. Int. Symp. (APSURSI)*, Charleston, SC, USA, Jun. 2009, pp. 1–4.
[40] B. Ravelo, "Distributed NGD active circuit for RF-microwave communication," *AEU-Int. J. Electron. Commun.*, vol. 68, no. 4, pp. 282–290, Apr. 2014.
[41] K.-P. Ahn, R. Ishikawa, and K. Honjo, "Group delay equalized UWB InGaP/GaAs HBT MMIC amplifier using negative group delay circuits," *IEEE Trans. Microw. Theory Techn.*, vol. 57, no. 9, pp. 2139–2147, Sep. 2009.
[42] H. Mirzaei and G. V. Eleftheriades, "Realizing non-foster reactances using negative-group-delay networks and applications to antennas," in *Proc. IEEE Radio Wireless Symp. (RWS)*, Newport Beach, CA, USA, Jan. 2014, pp. 58–60.
[43] W. Alomar and A. Mortazawi, "Elimination of beam squint in uniformly excited serially fed antenna arrays using negative group delay circuits," in *Proc. IEEE Int. Symp. Antennas Propag.*, Chicago, IL, USA, Jul. 2012, pp. 1–2.
[44] G. Chaudhary and Y. Jeong, "Transmission-type negative group delay networks using coupled line doublet structure," *IET Microw., Antennas Propag.*, vol. 9, no. 8, pp. 748–754, Jun. 2015.
[45] B. Ravelo, "Negative group-delay phenomenon analysis with distributed parallel interconnect line," *IEEE Trans. Electromagn. Compat.*, vol. 58, no. 2, pp. 573–580, Apr. 2016.
[46] B. Ravelo, "Theory of coupled line coupler-based negative group delay microwave circuit," *IEEE Trans. Microw. Theory Techn.*, vol. 64, no. 11, pp. 3604–3611, Nov. 2016.

FAYU WAN received the Ph.D. degree in electronic engineering from the University of Rouen, Rouen, France, in 2011. From 2011 to 2013, he was a Post-Doctoral Fellow with the Electromagnetic Compatibility Laboratory, Missouri University of Science and Technology, Rolla. He is currently a Full Professor at the Nanjing University of Information Science and Technology, Nanjing, China. His current research interests include negative group delay circuits, electrostatic discharge, electro-magnetic compatibility, and advanced RF measurement.

NINGDONG LI received the B.Sc. degree in electrical engineering from Anhui Polytechnic University, Wuhu, China, in 2017. He is currently pursuing the M.S. degree with the Nanjing University of Information Science and Technology, Nanjing, China. His research interests include abnormal wave propagation in dispersive media and microwave circuits.

BLAISE RAVELO received the Ph.D. degree from the University of Brest in 2008. His dissertation led to research [Habilitation á Diriger des Recherches (HDR)] from the University of Rouen in 2012. He is currently an Associate Professor at the Graduate Engineering School, ESIGELEC/IRSEEM, Rouen, France. His research interests cover the microwave circuit design, electromagnetic compatibility and interference, and signal and power integrity engineering. He is a pioneer of the negative group delay RF/analog and digital circuits, and systems. He is the (co)-author of over 200 papers and regularly involved in national/international research projects. He co-supervised and directed 9 Ph.D. students and 6 Ph.D. candidates who defended. He participates regularly in large R&D international projects. His current publication h-index is 16 (Reference: Google Scholar 2017).

Dr. Ravelo has been a URSI Member and regularly invited to review papers submitted to international journals (the IEEE TMTT, the IEEE Access, the IEEE TCS, the IEEE TEMC, the IEEE TIM, the IEEE TIE, the *Journal of Electromagnetic Waves and Applications*, the IET CDS, the IET MAP, and the *International Journal of Electronics*) and international books (Wiley and Intech Science). He is the Scientific Chair of the 5th International Conference on Electromagnetic Near Field Characterization and Imaging in 2011, a member of the Advanced Electromagnetic Symposium 2013-2018 Technical Committee and the IEEE RADIO 2015 Scientific Committee.

QIZHENG JI received the M.S. degree in aircraft design from the China Academy of Space Technology (CAST), Beijing, China, in 2006. He is currently a Senior Engineer in technology and management of electrostatic protection with the Beijing Orient Institute of Measurement and Test, CAST. His research interests include microwave circuits and ESD.

JUNXIANG GE received the Ph.D. degree in radio engineering from Southeast University, Nanjing, China, in 1991.

He has been the Dean of the School of Electronic and Information Engineering, Nanjing University of Information Science and Technology, Nanjing, since 2011. His current research interests include electromagnetic field theory, microwave and millimeter wave technology, and antenna.